Supporting Information

Flexible, transparent, and sustainable cellulose-based films for organic solar cells substrates

Lewen Huang‡ [a], Yibao Li[a], , Zhong Zheng[b], Yun Bai[a], Thomas P. Russell[c,d] and Changfei He[‡a*]*

‡ These authors contributed equally.

*corresponding author

a School of Chemistry and Chemical Engineering, ，Gannan Normal University，341000，Ganzhou, China.

b School of Chemistry and Biology Engineering, University of Science and Technology Beijing, Beijing 100083, China.

c Materials Sciences Division, Lawrence Berkeley National Laboratory, 1 Cyclotron Road, Berkeley, California 94720, United States

d Polymer Science and Engineering Department, University of Massachusetts Amherst, Amherst, Massachusetts 01003, United States

1. Calculation the degree of substitution of m-Cell .

The degree of substitution(D_S) of m-MCC was calculated lowing equation according to the ^{1}H NMR spectra. (Figure S14)

$$\frac{m_{BR} / M_{BR}}{m_{m-Cell} / M_{m-Cell}} = \frac{I_{BR}}{I_{m-Cell}} D_s \qquad (1)$$

$$M_{m-Cell} = 162 + 166.22 D_s \qquad (2)$$

Where m_{BR} and M_{BR} is the mass and molecular weight of BR as a reference, m_{m-Cell} and M_{m-Cell} is the mass and average molecular weight of m-Cell. I_{BR} and I_{m-Cell}, is the integral area of peak a and peak 16 and 17. constant 162 is the molecular weight of unit of the anhydroglucose unit, constant 166.22 is the molecular weight of 10-undecenoyl chloride subtracting 36.5 (molecular weight of hydrogen chloride). The average of D_S is 1.25 through twice test.

2. Preparation cellulose film

The procedure for preparation cellulose films as follows: MCC (4g, 5wt%) was dried at 105 °C for 2 h. AMIMCl (76 g, 95wt%) was added in 250 mL Shrek bottle and heat up to 80 °C in an oil bath, and then MCC was added in it. After stirring 30min, the MCC solution (30 mL) was casting on the glass (ca. 150mm(L) × 150mm(W) ×5.0mm(T)). and immersed in water. The obtained cellulose gel was washed with water until all solvents was removed, and then dried at room temperature in a ventilated place.

3. The fabrication of OSCs

The CV-20/ITO substrates were fabricated by sputtering ITO on CV-20. During sputtering, the temperature of ITO target was kept at about 200 ℃. After sputtering, the ITO coated CV-20 can be directly used for device fabrication without additional annealing. PEN/ITO or CV-20/ITO substrates were cleaned with detergent, deionized (DI) water, acetone and isopropanol. After 5 min UV-ozone, the ITO substrates were cooled down for further using. By using PDMS bonding technology, the flexible substrates were attached onto rigid glasses for further spin coating. For conventional

OSCs, the emulsion of PEDOT:PSS (CLEVIOS P VP AI 4083) was spin coated on top of the fixed substrates with 4000 rpm and then annealing were carried out. After annealing, the PEDOT:PSS coated ITO substrates were transferred into N2 glove box. Then the solutions of BHJ were spin coated or blade coated based on the used conditions. Then the BHJs should be annealed. After thermal annealing, the PDINN layer was spin coated with 3000 rpm. After that 200 nm of Ag were thermally evaporated under high vacuum (ca. 3×10-4 Pa). For inverted OSCs, the precursor sol of ZnO was spin coated on top of the fixed substrates with 3000 rpm and then annealing were carried out in air with 60% relative humidity. After annealing, the ZnO coated ITO substrates were transferred into N2 glove box. Then the solutions of BHJ were spin coated or blade coated based on the used conditions. Then the BHJs should be annealed. After thermal annealing, 7 nm-thick MoO3 layer should be fabricated on the surfaces of the BHJs by vacuum evaporation. After that 200 nm of Ag were thermally evaporated under high vacuum (ca. 3×10-4 Pa). The cell area was 0.0223 cm2 which are defined by apertures.

4. The formula of CVs

Table S1. Formula for preparation CV films.

Samples	Weight of m-Cell/g	C=C/eqv.	Weight of BDB/g	BDB/eqv.
CV-10	1.00	1.00	0.10	0.12
CV-20	1.00	1.00	0.20	0.25
CV-30	1.00	1.00	0.30	0.37

5. The Characterization of CVs

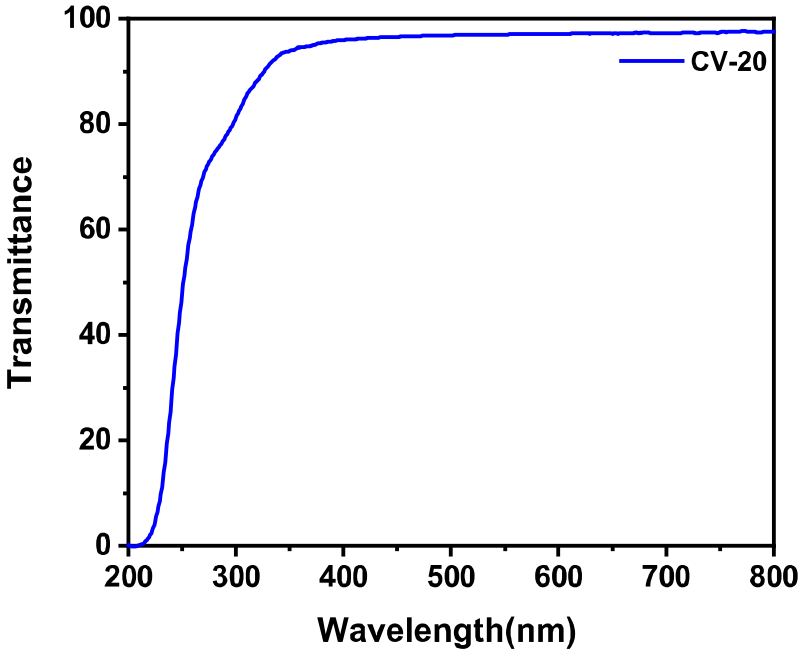

Figure S1. The UV-vis spectra of CV-20

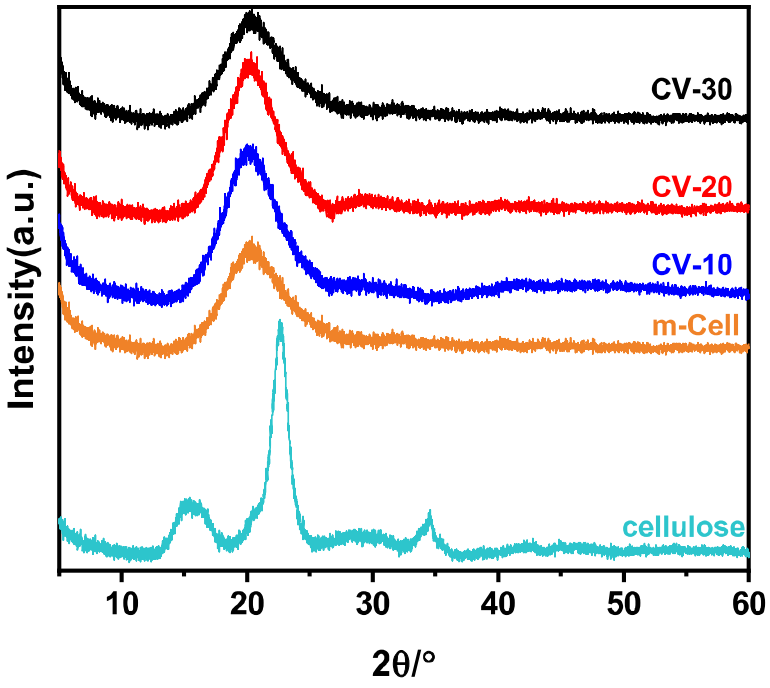

Figure S2. XRD spectra of CVs and m-Cell.

Table S2. Mechanical strength of CVs and cellulose

Samples	Elasticity moduluse(Mpa)	Stress(MPa)	Strain(%)
m-Cell	395.63±14.01	20.46±0.58	69.26±4.34
CV-10	845.02±15.20	46.97±4.00	39.75±5.66
CV-20	965.57±71.46	53.67±4.94	24.29±3.00
CV-30	1379.29±90.13	60.33±2.53	16.44±2.31
cellulose	4009.05±469.31	63.68±7.99	8.59±1.21

Table S3. Mechanical strength of CVs and cellulose soaking in H_2O for 30 min

Samples	Elasticity moduluse(Mpa)	Stress(MPa)	Strain(%)
CV-10	641.45±34.13	28.13±0.80	49.57±6.26
CV-20	953.33±10.89	38.58±4.35	29.31±9.08
CV-30	1270.55±31.66	53.82±4.30	22.29±4.39
cellulose	94.83±11.48	7.94±2.18	16.13±2.90

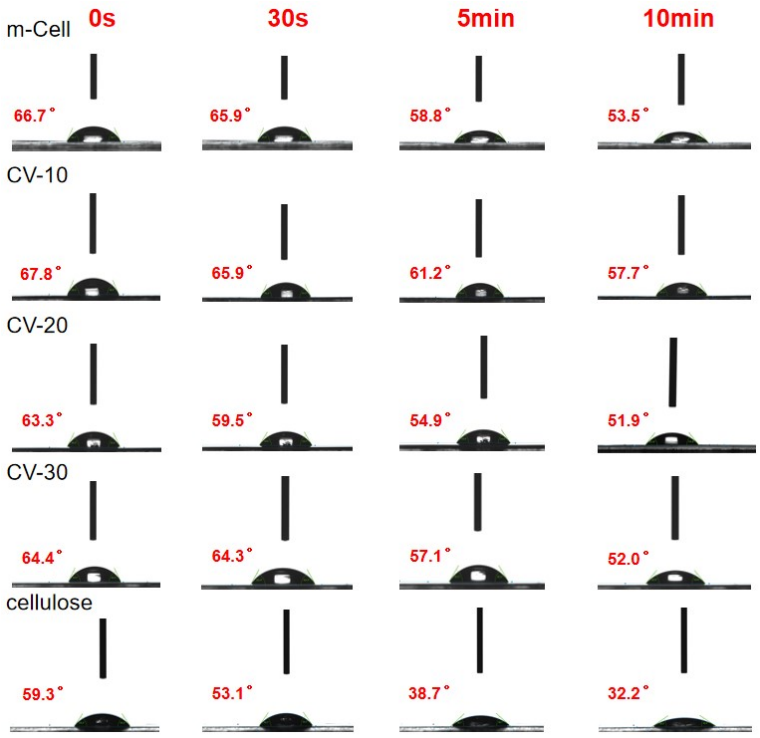

Figure S3. Comparison of water contact angle of CVs and cellulose film during 10min.

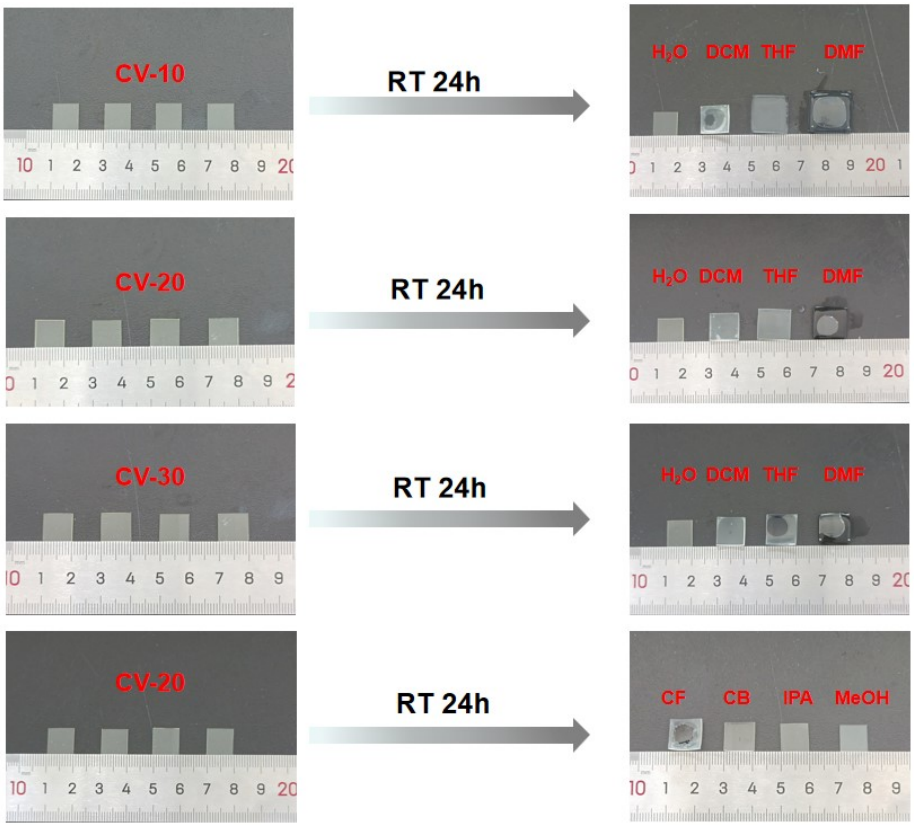

Figure S4. The shape stability of CVs after immersing in different solvents for 24 h at room temperature.

Table S4. Gel fraction of CVs after soak in different solvents for 24 h at room temperature

Solvents	CV-10	CV-20	CV-30
	Content(%)	Content(%)	Content(%)
H_2O	99.43	99.34	98.98
DCM	96.90	97.23	97.12
THF	93.14	95.13	95.70
DMF	88.71	95.45	96.75
CB	/	99.44	/
CF	/	99.27	/
IPA	/	99.64	/
MeOH	/	99.62	/

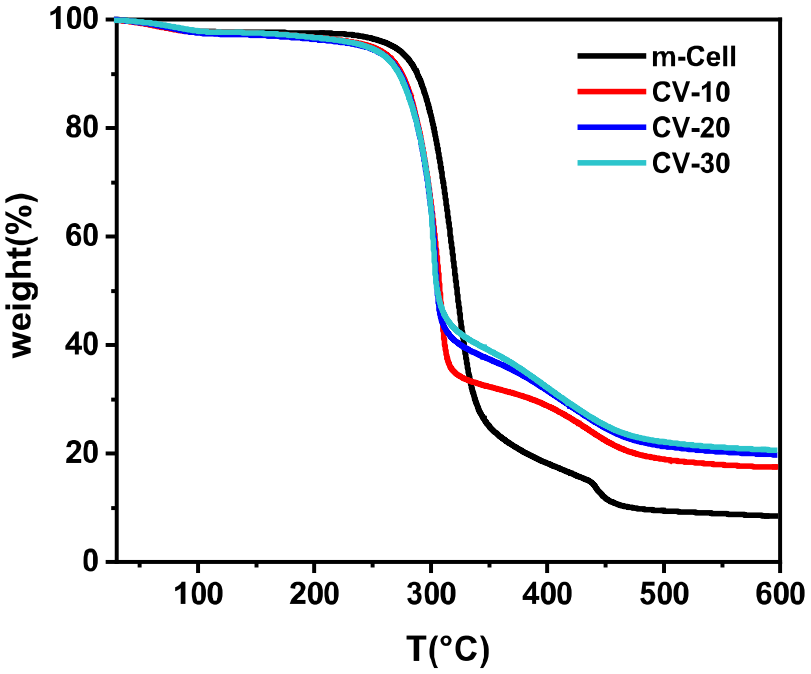

Figure S5. TGA of CVs and m-Cell at 10 °C min^{-1} under N_2.

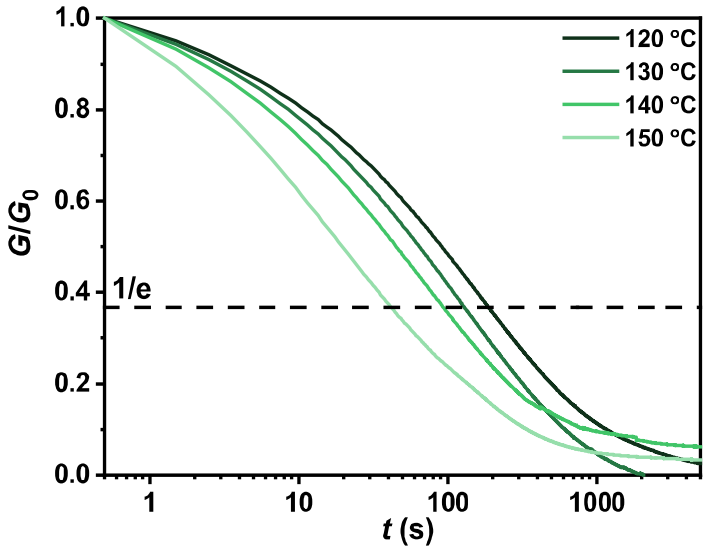

Figure S6. Normalized stress-relaxation curves at different temperates for CV-10.

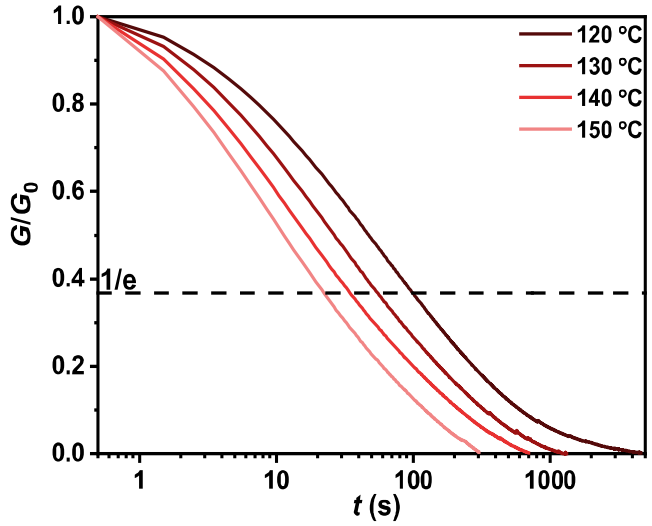

Figure S7. Normalized stress-relaxation curves at different temperates for CV-30.

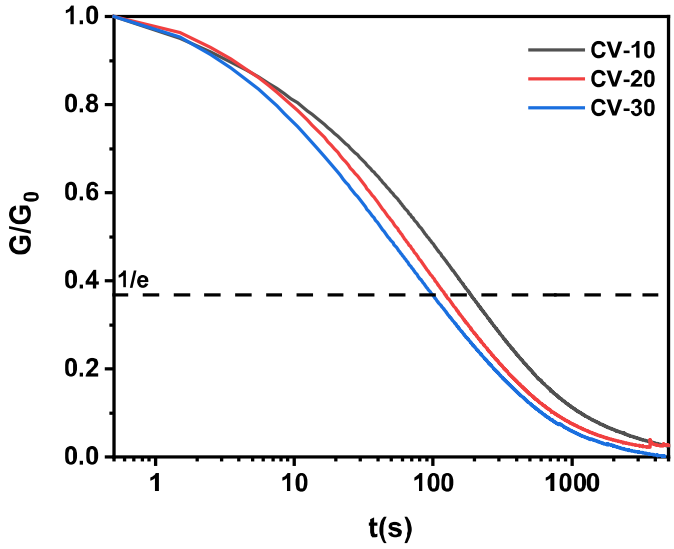

Figure S8. Normalized stress-relaxation curves of CVs at 120 ºC.

Table S5. Mechanical strength of recycled CV-20

CV-20	Young's moduluse(Mpa)	Stress(MPa)	Strain(%)
Original	965.57±71.46	53.67±4.94	24.29±3.00
1st recycled	911.95±105.29	55.68±4.22	36.52±4.52
2nd recycled	1033.81±22.90	48.30±7.37	26.60±6.39
3rd recycled	974.59±107.04	50.07±8.84	33.75±9.64
4th recycled	1224.91±118.36	50.81±3.63	29.72±5.49

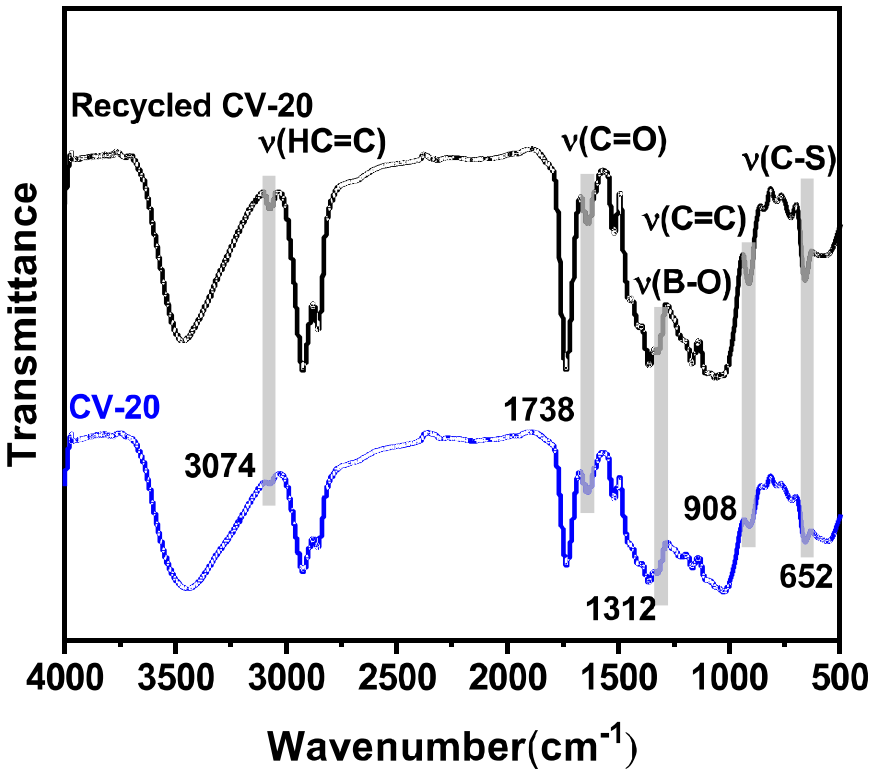

Figure S10. FT-IR spectra of CV-20 and recycled CV-20

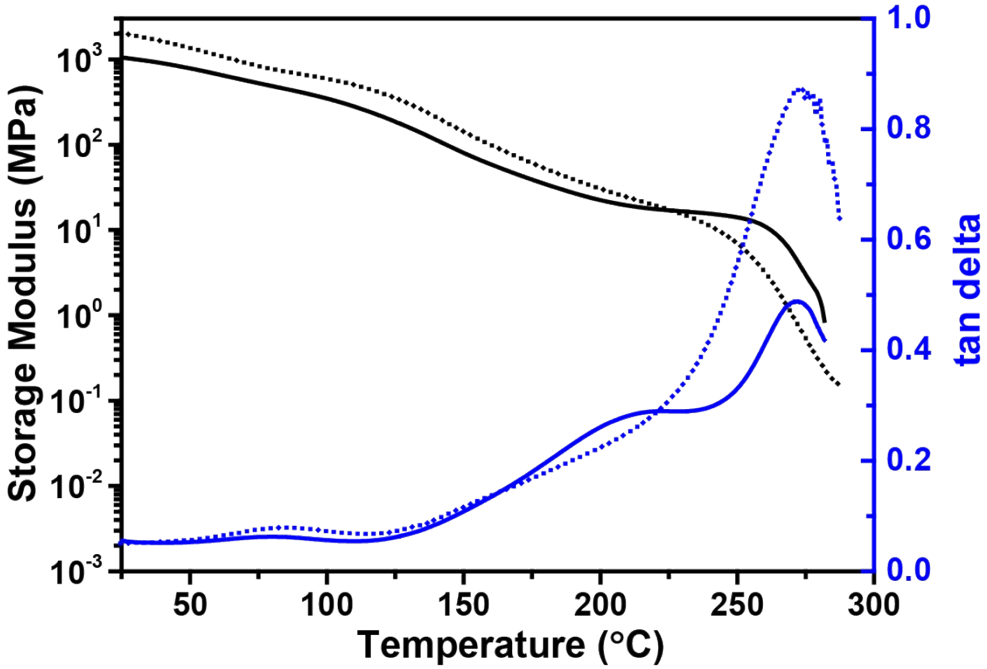

Figure S11. DMA curves of CV-20 (solid) and recycled CV-20 (dot).

Table S6. Device performance of OSCs employing CV-20 and PEN as substrates.

OSCs		V_{oc}[a] (V)	J_{sc}[b] (mA/cm^2)	FF (%)	PCE (%)
Conventional	PEN	0.86	26.07	63.34	14.20
	CV-20	0.86	26.67	75.21	17.25
Inverted	PEN	0.74	24.54	60.30	10.95
	PEN	0.82	26.50	71.24	15.48
	PEN	0.82	26.77	75.32	16.13
	CV-20	0.84	26.43	75.76	16.82
	CV-20	0.85	26.66	76.61	17.36
	CV-20	0.83	26.83	74.72	16.64

[a]V_{oc} refers to open-circuit voltage. [b]J_{sc} refers to short-circuit current density.

Table S7. Summary of PV devices fabricated on cellulose substrates

Technology	**substrates**	**T_g (°C)**	**Tensile strength (MPa)**	**Transmittance (%)**	**Thickness (μm)**	**PCE%**	**Ref.**
OPV	**CV-20**	**272**	**53**	**92**	**15-80**	**17.2**	**this work**
	CNC	-	-	75	18-30	2.4	1
	CNC	-	-	-	-	4	2
	CNC	-		81	45-50	1.4	3
	TOCN	-	70.1	78.5	50-60	7.47	4
	DHPC/DCNC	-	16	85	100	4.98	5
	ACNF-Epoxy	71.8	68	89	30		6
	paper	-	-	-	-	4.1	7
	NFC	-	-	90	-	0.4	8
	Cellophane	-	50	91	25	5.94	9
PSC	cellulose	-	-	-	-	2.7	10
	TEMPO-oxidized cellulose	-	-	80	20	6.37	11
	Cellulose	-	-	70	-	9.05	12
	NCP/Acrylic resin	-	81	91.7	43.5	4.25	13

(-)not supplied

6. NMR spectra

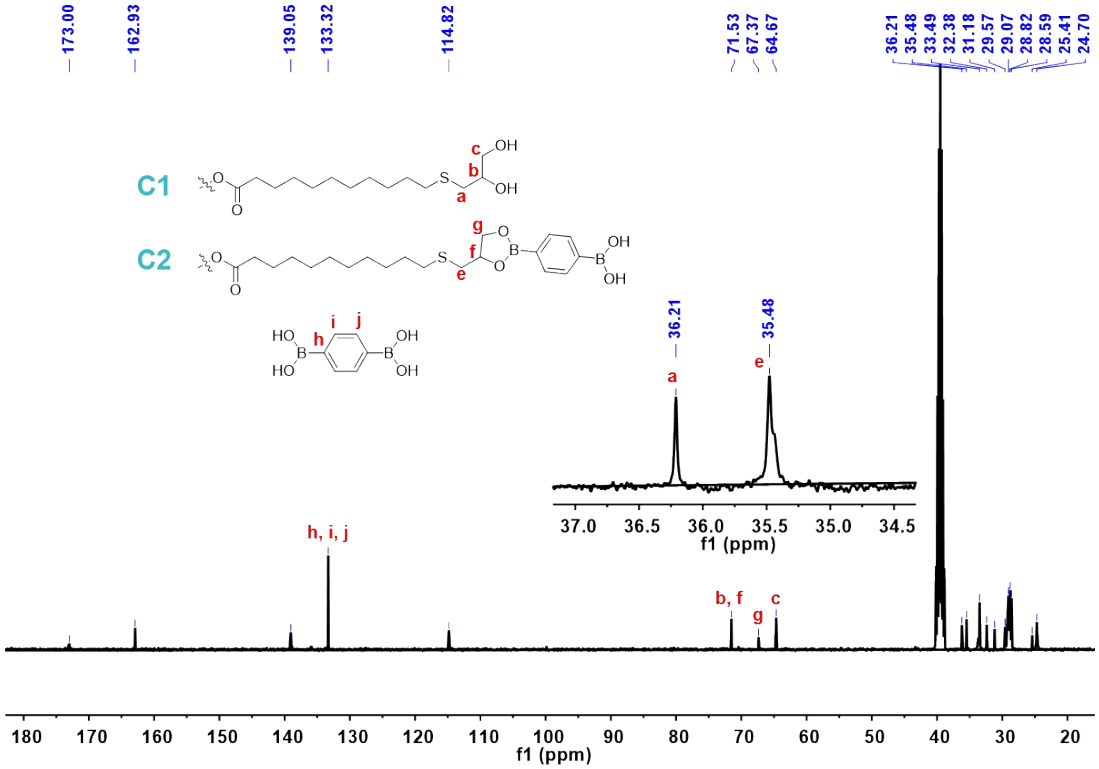

Figure S12. ^{13}C NMR spactra of CV-20 dissovled in DMSO-d6

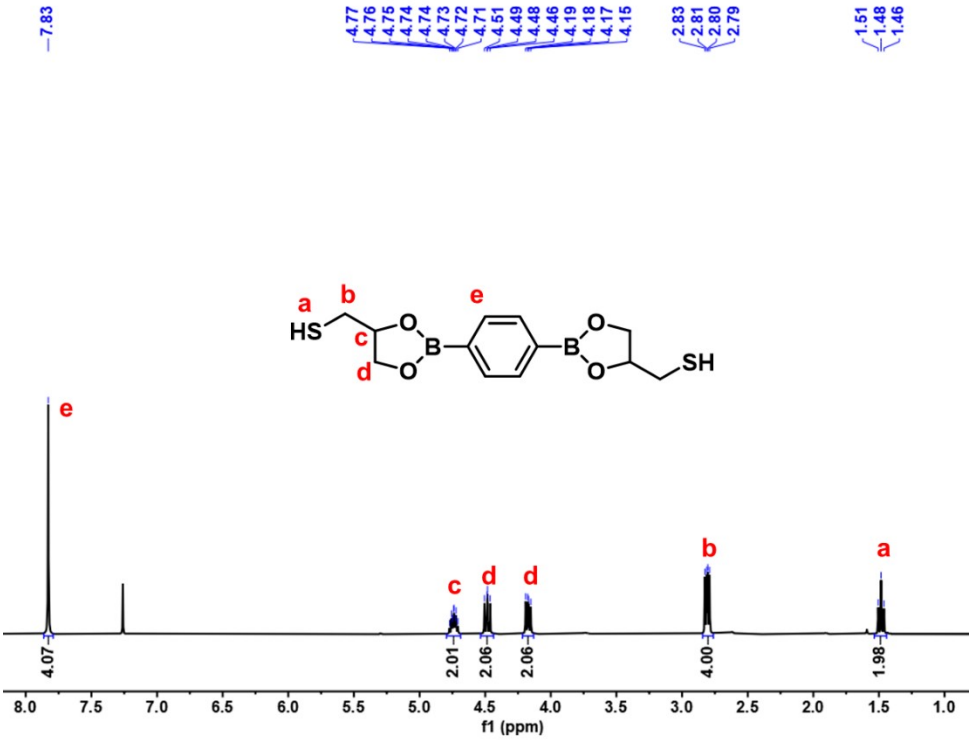

Figure S13. ^{1}H-NMR spactra of BDB.

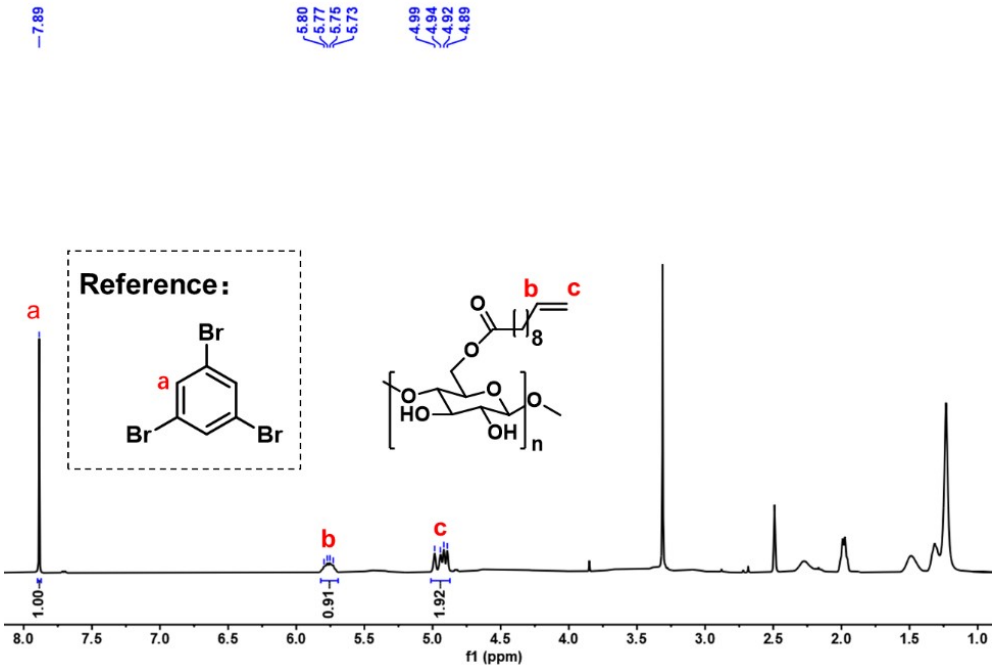

Figure S14. ^{1}H NMR spectra of m-Cell with a reference.

Reference

1. Y. Zhou, C. Fuentes-Hernandez, T. M. Khan, J. C. Liu, J. Hsu, J. W. Shim, A. Dindar, J. P. Youngblood, R. J. Moon, B. Kippelen, *SCI REP-UK* **2013**, *3*, 1536.

2. Y. Zhou, T. M. Khan, J. C. Liu, C. Fuentes-Hernandez, J. W. Shim, E. Najafabadi, J. P. Youngblood, R. J. Moon, B. Kippelen, *ORG ELECTRON* **2014**, *15*, 661-666.

3. S. V. Costa, P. Pingel, S. Janietz, A. F. Nogueira, *J. APPL. POLYM.* SCI. **2016**, *133*, 28.

4. P. C. Lin, C. T. Hsieh, X. Liu, F. C. Chang, W. C. Chen, J. Yu, C. C. Chueh, *Chem. Eng. J.* **2021**, *405*, 126996.

5. Q. Cheng, D. Ye, W. Yang, S. Zhang, H. Chen, C. Chang, L. Zhang, *ACS Sustainable Chem. Eng.* **2018**, *6*, 8040-8047.

6. R. Wang, H. Yu, M. Dirican, L. Chen, D. Fang, Y. Tian, C. Yan, J. Xie, D. Jia, H. Jia, H. Liu, J. Wang, F. Tang, A. M. Asiri, X. Zhang, J. Tao, *ACS Appl. Energy Mater.* **2020**, *3*, 785−793.

7. L. Leonat, M. S. White, E. D. Glowacki, M. C. Scharber, T. Zillger, J. Rübler, N. S. Sariciftci, *J. Phys. Chem. C* **2014**, *118*, 16813–16817.

8. L. Hu, G. Zheng, J. Yao, N. Liu, B. Weil, M. Eskilsson, E. Karabulut, Z. Ruan, S. Fan, J. T. Bloking, M. D. McGehee, L. Wågberg, Y. Cui, *Energy Environ. Sci.*, **2013**, *6*, 513-518.

9. H. Li, X. Liu, W. Wang, Y. Lu, J. Huang, J. Li, J. Xu, P. Fan, J. Fang, W. Song, *Solar. RRL* **2018**, *2*, 10.

10. S. Castro-Hermosa, J. Dagar, A. Marsella, T. M. Brown, *IEEE Electron Device Letters* **2017**, *38*, 9.

11. M. H. Jung, N. M. Park, S. Y. Lee, *SOL ENERGY* **2016**, *139*, 458-466.

12. C. Gao, S. Yuan, K. Cui, Z. Qiu, S. Ge, B. Cao, J. Yu, *Solar. RRL* **2018**, *2*, 11.

13. L. Gao, L. Chao, M. Hou, J. Liang, Y. Chen, H. D. Yu, W. Huang, *npj Flex. Electron.* 2019, 3, 4.